SOILS AND FOUNDATIONS Vol. 48, No. 3, 319–332, June 2008
Japanese Geotechnical Society

CYCLIC TRIAXIAL TESTS ON ASPHALT CONCRETE AS A WATER BARRIER FOR EMBANKMENT DAMS

Siamak Feizi-Khankandi[i], Ali Asghar Mirghasemi[ii], Abbas Ghalandarzadeh[iii] and Kaare Hoeg[iv]

ABSTRACT

The seismic behavior of asphaltic concrete used in embankment dams subjected earthquake loads has been studied. In order to evaluate the dynamic behavior, an extensive series of monotonic and cyclic tests were carried out on triaxial specimens of asphalt concrete used in hydraulic structures. The MTS-dynamic equipment at the Norwegian Geotechnical Institute (NGI) was used for this purpose. Temperature and frequency effects on specimen behavior and on specimen degradation have been studied under the cyclic loads in both isotropic and anisotropic initial stress conditions. For investigation of the fatigue behavior, thousands of cyclic loads were imposed on some of the specimens. Moreover, to study any sign of material degradation due to the cyclic loading, the post-cyclic monotonic stress-strain curve was compared with the corresponding curve for specimens that were not first subjected to cyclic loading. Geotechnical parameters to be used in dynamic numerical analysis models are also presented.

Key words: asphaltic concrete core dams, cyclic tests, monotonic tests, seismic behavior (**IGC**: H4/M3)

INTRODUCTION

The sealing of earth and embankment dams by means of asphalt concrete cores has attained importance throughout the world. This kind of material is virtually impervious, flexible, and resistant to erosion and aging and exhibits visco-elastoplastic behavior (ICOLD, 1992; Hoeg et al., 2007). In regions with cold and rainy weather, construction of this kind of dam is easier than that of clay core dams. For many years, monitoring of these dams has indicated their suitable behavior during construction and operation. However, little information exists on the behaviour of asphalt concrete core dams subjected to seismic loads. There are only a few published documents providing information on the behavior of asphalt concrete used as impervious water barriers in dams during and after earthquake shaking.

Previous Numerical Studies

Valstad et al. (1991) analyzed the Storvatn dam located in Norway using a Newmark approach to compute the earthquake induced permanent displacements along the critical sliding surfaces. They studied whether the permanent shear displacements of a dam due to severe shaking may be so great that a thin core may be sheared off toward the dam crest.

Hoeg (1993, 2005) presented the results of Storvatn dam and showed that relatively large shear strains may occur in the top of the core if the dam slopes are very steep. However, he concluded that rockfill dams with asphaltic concrete core in general have a favorable seismic protection.

Meintjes and Jones (1999) analyzed the Ceres dam located in South Africa. They also used the Newmark method to estimate permanent shear displacements. The predicted behavior of the dam was satisfactory.

Gurdil (1999) performed seismic analyses the Kopru dam in Turkey. His analyses were based on the equivalent linear method. He concluded that some cracking may occur in the core, near the crest level. However, the self healing behavior of asphaltic concrete will solve this problem.

Ghanooni and Mahin-roosta (2002) performed dynamic analyses on a typical 115 m high asphaltic concrete core rockfill dam. They concluded that, in nonlinear analyses, the top section of the core experiences small tensile stresses which are less than asphalt material strength.

Feizi-Khankandi et al. (2004) performed a 3-*D* analysis on a typical 60 m high asphaltic concrete core dam. They concluded that as in the case of 2-*D* analysis, the top section of the core experiences some tensile stresses, but somewhat more than in the 2-*D* analysis. Furthermore, they concluded that although there is a possibility of some cracking in the top of the asphaltic core, the dam

[i] Ph.D. Student, School of Civil Eng., College of Engineering, University of Tehran, Iran (sfeizi@ut.ac.ir).
[ii] Associate Professor, ditto (aghasemi@ut.ac.ir).
[iii] Assistant Professor, ditto (aghaland@ut.ac.ir).
[iv] Professor, Norwegian Geotechnical Institute (NGI) and University Of Oslo Norway (kaare.hoeg@ngi.no).
The manuscript for this paper was received for review on March 5, 2007; approved on February 14, 2008.
Written discussions on this paper should be submitted before January 1, 2009 to the Japanese Geotechnical Society, 4-38-2, Sengoku, Bunkyo-ku, Tokyo 112-0011, Japan. Upon request the closing date may be extended one month.

could be designed to behave safely.

Previous Experimental Work

The first experimental research in the field of seismic behavior of asphaltic concrete core dams was performed by Breth and Schwab (1973). Their study was based on finite element analysis of a dam with a height of 180 m. They devised an interesting set-up to impose computed cyclic horizontal shear stresses on representative elements of the asphaltic concrete core. They concluded that the cyclic loads did not change the structural strength of the asphalt concrete which behaved like an elastic body.

Ohne et al. (2002) performed one-way uniaxial cyclic tests on the specimens drilled out from Higashifuji dam in Japan (the asphaltic concrete face dam was damaged by an earthquake in 1996). Twenty stress cycles were applied at each static stress level. They defined the dynamic yield strain for the asphalt material. The authors concluded that the observed cracks that opened in the facing of the dam were caused by cyclic compression stresses.

Wang (2005) reported a series of cyclic loading tests on triaxial specimens of asphaltic concrete. He showed that there was no sign of cracking or degradation of the specimens.

Salemi (2005) performed some numerical and experimental tests for Meyjaran dam in Iran with a height of 60 m. Small scale physical models of asphalt core dams were also tested in a centrifuge under impact loads. She concluded that her numerical analysis corresponded well with data recorded in the model and mentioned that the asphalt-concrete core behaves safely, even under a very severe earthquake.

It is important to determine the level of tensile stress and the amount of tensile strain that asphalt concrete in a dam core can sustain before it cracks. This strain level is clearly a function of temperature and rate of loading. In earthquake prone regions, the asphalt concrete mix is usually made with a soft grade bitumen and/or an added (0.5–1)% bitumen content to increase the flexibility and ductility and the tensile cracking strain (Hoeg et al., 2007).

The tensile or breaking strength of asphalt concrete decreases with the time of loading or with the increase in temperature. The tensile strength of an asphalt mix is of the order of 10% of the compression strength of the asphalt concrete (Creegan and Monismith, 1996). The most recent paper discussing the tensile strength and tensile cracking strain is the one presented by Nakamura et al. (2004). The main goal of their study was to compare the engineering properties of conventional asphalt concrete with a special admixture (called Superflex-phalt). The Superflex-phalt has a much lower tensile strength and a higher tensile cracking strain than conventional asphalt concrete used in hydraulic structures.

PURPOSE AND SCOPE OF THE PRESENT RESEARCH

Many researches have been done on the asphalt concrete on the road and airfield pavements. However, on the water barrier for hydraulic structures such asphaltic concrete core or face dams, there is not much research in the literature about the behavior of asphalt concrete, especially during an earthquake occurrence.

To investigate the stress-strain behavior of asphalt concrete under static and dynamic loads and for determination of geotechnical parameters of this material, monotonic and cyclic tests were performed. At least 50 and at most 10000 cycles were applied to the samples in different confining pressures, temperatures and frequencies. The tests were done in both isotropic and anisotropic conditions. In addition, some monotonic tests were carried out before and after cyclic tests to investigate post-cyclic behavior of asphalt concrete and loading effect on the material strength.

In this research, the laboratory investigations are divided into three sections. In the first, monotonic tests were performed to determine stress-strain behavior of the asphalt concrete before application of the cyclic loads. Triaxial cyclic tests in both isotropic and anisotropic conditions were carried out in the second part of this study. Performing monotonic tests after application of the cyclic loads, to compare the results with first section was the third part of the study.

Briefly, the following topics form the main scope of the present experiment:

- Material degradation due to cyclic loading (specially after 50 cycles)
- Effects of different parameters on the behaviour of specimens
- Possible cracking of samples due to cyclic loads
- Behaviour of specimens under thousands of cyclic loads
- Determination of geotechnical parameters to be used in the numerical analysis
- Post-cyclic behaviour of asphalt concrete

PREPARATION OF THE ASPHALT CONCRETE SPECIMENTS

All specimens were prepared in the asphalt laboratory of Kolo-Veidekke in Norway. Firstly, small size specimens were prepared based on the standardized Marshal method. The size distribution of the sand and gravel in the asphalt concrete mix complied with the Fuller's equation (Hoeg, 1993; Creegan and Monismith, 1996):

$$P_i = 100\left(\frac{d_i}{d_{max}}\right)^{0.41}\% \quad (1)$$

Where: P_i is the percent by weight smaller than the equivalent grain size dimension d_i. These initial tests were accomplished to reach the optimum percent of the bitumen value to mix with the aggregates. The used bitumen was of grade B60 and the tests were done with the bitumen percentages by weight of 5, 6, 6.5, 7 and 7.5. The type of asphalt binder used is important, because the shear modulus and the damping ratio are dependent on the properties of asphalt binders as well. There is a wide

range of bitumen grades to be chosen for hydraulic asphalt concrete. The asphalt binder type selection depends on specific project conditions and behavior requirements of asphalt concrete including its degree of penetration.

Based on the Marshal's test results, the value of 7.0 percent by weight was selected for the mix. The laboratory triaxial specimens were prepared in a mould with a diameter of 100 mm and a height of 200 mm. Dry aggregates and the added filler, in accordance with the calculated weight based on Fuller's equation were put inside the oven to reach a temperature of 152°C. Besides, bitumen was put inside another oven for preheating and to reach a temperature of 145°C (Baron et al., 1955). Both of these materials remained inside the oven for ten hours. After this period, the calculated weight for bitumen was added to the aggregates and then placed in a mixer for nearly three minutes. A standard Marshall tamping hammer was used with 30 blows per layer for compaction of the samples (one blow per second). This hammer has a weight of 4.5 kg and the height of its drop is 45 cm. The specimens were built in four layers of equal thickness. Air void of all samples was obtained to be less than 1%. Wang and Hoeg (2002) showed that this compaction procedure gives specimens that have the same compressive strength, but a somewhat higher compression modulus than field specimens drilled out of a dam core compacted by a light vibratory roller.

Later on, the samples were trimmed with a special saw to a length of 200 mm. During trimming of specimens, a very high sensitive trimmer was used and the surface of the samples were cut and polished with very high degree of precision to decrease the bedding error effect during the tests. Figure 1 shows prepared samples for an example. Flatness, roughness and parallelism for the specimen ends had the ability to satisfy the suggested criteria by Japanese Geotechnical Society, 2000 and ASTM D 3999–91.

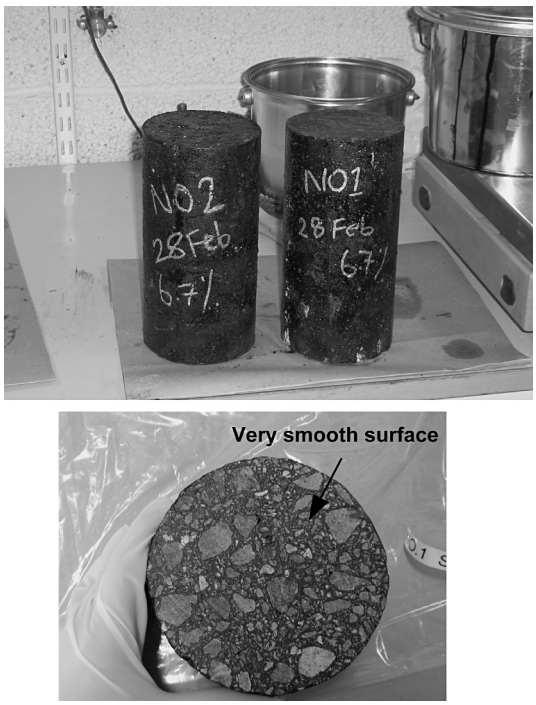

Fig. 1. Picture of prepared samples

MONOTONIC TRIAXIAL TESTS

Monotonic triaxial compression tests were used to study the stress-strain-strength behavior of asphalt concrete. Six monotonic tests were performed in different confining pressures (Table 1). All prepared specimens were put inside the cooling room with temperature of 5°C before starting the monotonic tests. Specimens were taken from the cooling room and were set up within a triaxial cell. In all tests, there were membranes used around the specimens. The triaxial cell was filled with deaerated water and then the equipment was put inside a big cell used to retain a constant temperature during the test. All monotonic tests were performed by use of strain-controlled compression loading system. After applying the predefined confining pressure and reaching to a constant temperature, the axial load was applied up to the failure point. The imposed axial strain rate was 2% per hour. All tests were continued to a very large axial strain (about 20%). At that stage, the specimens had a pronounced barrel shape and were seriously cracked. During the test, the amount of axial stress, axial strain and volumetric strain were recorded by the electronic sensors used for this purpose.

Presentation of the Results

Table 1 presents the summary of results for monotonic triaxial tests. Figures 2 and 3 show the values of deviator stress and volumetric strain versus axial strain for imposed confining pressures (250, 500 and 1000 kPa). For all confining pressures, the same stress-strain trend is seen in Fig. 2. As expected, the higher is the value of confining pressure, the more is the amount of failure axial strain. Values of axial strain at failure point for $\sigma_3 = 1000$, 500 and 250 kPa are 15, 6 and 5 percent respectively. Also, the curves show a good harmony between two repeated tests in the same confining pressures. This similarity is even more evident in higher confining pressures. This is because, with the increasing confining pressure, the samples, to some extent, behave like rigid materials.

Equivalent Young modulus (E) was derived from the initial stage of the curve, up to an axial strain of 1%:

Table 1. Results of monotonic triaxial tests

Test No.	σ_3 (kPa)	E (MPa)	σ_1-σ_3 (kPa) at failure	Temperature (°C)	Axial strain at failure (%)
T1	250	135	2522	5	5.5
T2	250	110	2197		5.5
T3	500	150	3129		6
T4	500	150	3332		6
T5	1000	160	3879		15
T6	1000	150	3793		15

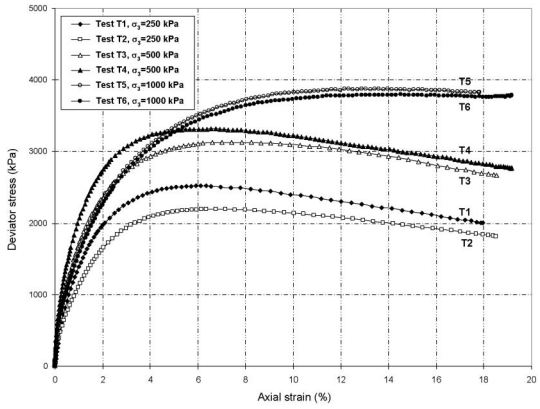

Fig. 2. Deviator stress- axial strain curves

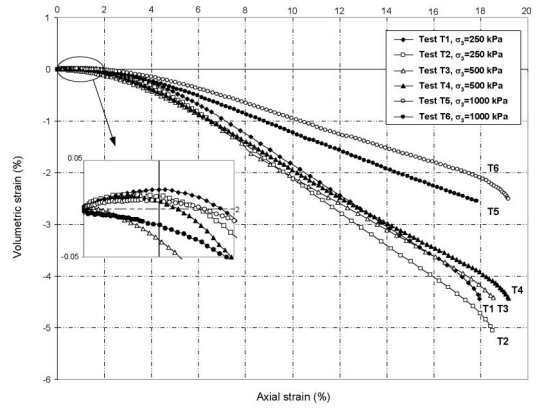

Fig. 3. Degree of dilatancy as a function of confining pressure

$$E = \frac{\sigma_d}{\varepsilon_a} \tag{2}$$

For confining pressures of 250 to 1000 kPa, the range of the secant modulus is between 110 MPa and 150 MPa (Table 1).

As previously known, the value of elasticity modulus is a function of many parameters like porosity and confining pressure (Kramer, 1996). In other words:

$$E_{1\%} = f(e, \sigma_0', \ldots) = K \times f(e) \times f(\sigma_0') \tag{3}$$

where: K is a constant parameter and e is the specimen void ratio.

In all specimens, the amount of void ratio is less than 1%. Therefore:

$$E_{1\%} = A \times \sigma_0^y \tag{4}$$

where: A is a constant parameter.

Based on the monotonic tests results (Fig. 2), the value of y in the above relation is calculated and the following equation is defined for asphalt concrete materials:

$$E_{1\%} = A \times \sigma_0^{0.18} \tag{5}$$

Young modulus for asphalt concrete does not show a substantial increase while increasing the confining stress. This is in contrast with the results from triaxial samples of the aggregate alone, which show a modulus increasing markedly with increasing confining pressures. However, for the strain values more than 1%, a significant increase in shear strength is observed while increasing confining pressures.

To study the effect of reduction of bitumen viscosity, supplementary triaxial tests results were reported by Hoeg, 1993. The results showed that the same geotechnical parameters are observed with 5.9% B180 and 8% B60.

Figure 3 shows the relation between volumetric and axial strains. The results show that with the increase in the confining pressure, the value of dilatancy decreases. Up to an axial strain of 3%, however, the amount of dilatancy is small, e.g., less than 0.5%. Moreover, this figure shows a very little volumetric compression at the initial stage of the tests. It is quite common, as in the first seconds after the load application; little spaces existing inside the specimens raze. After a few seconds, the volume shows expansion. This important phenomenon is due to the opening of small fissures. Although no visible cracks may appear, the dilatation may lead to an increase in permeability. However, the increase in permeability only occurs when fissures get opened in consequence of shear deformations at a stress level which causes specimen failure.

TRIAXIAL TESTS WITH CYCLIC LOADING

Twenty-four cyclic triaxial tests were carried out in this research (Table 2). The specimens were loaded under initial isotropic condition ($k_c = \sigma_1/\sigma_3 = 1.0$) and anisotropic conditions ($k_c = 2.0$ and 3.0). During the tests, the amount of anisotropy coefficient was fixed by applying the desired loads from the load cell of triaxial equipment. The confining pressure was varied from 85 kPa to 500 kPa. As the behavior of the asphaltic concrete core near the top of the dam is of most concern when it is subjected to the cyclic loads of earthquake, this range of confining stress was selected. The cell pressure was generated by the pressurized de-aired water where the cell was fully under computer controlled data acquisition system.

The specimens with rubber membranes were placed in the triaxial cell and then subjected to a confining pressure. Moreover, the triaxial cell was put inside a bigger cell connected to a water pumping system. This system had the capability of applying any temperature to the pumped water. In the duration of 12 hours, the temperature gradually reached a predefined value. All tests were performed at two different temperatures, $T = 5°C$ and $T = 18°C$. These temperatures were chosen from the temperature monitoring of the embankment dams (Dannicliff, 1996). Conditions inside a dam will be rather constant, and selected temperatures to cover some typical variation, were set to $T = 5°C$ and $T = 18°C$; $T = 5°C$, as an assumed year-around temperature inside a typical dam in sun-arctic climate and $T = 18°C$, as an assumed year-around temperature inside dam in countries with tropical or sub-tropical climate. On the other hand, in embank-

Table 2. Summarized information of cyclic triaxial tests

Test No.	σ_3 (kPa)	K_c	T °C	Frequency (Hz)	Number of cycles	G (GPa)	Type of loading
F1	500	1	5	2	50	1.80	A
F2	500	1	5	2	50	1.75	A
F3	500	2	5	2	50	2.50	B
F4	500	2	5	2	50	2.30	B
T5	250	1	5	2	50	1.40	A
T6	250	2	5	2	50	1.67	B
T7	250	3	5	2	50	1.70	B
T8	250	2	5	2	50	1.72	B and C
F9	500	1	5	2	50, 400, 50	2.00	A
F11	500	3	5	2	50, 10000	3.75	B
E12	85	1	5	2 and 10	50, 2000, 50	1.30	A
E13	85	2	5	2 and 10	50, 1000, 1000, 50	1.33	B
F14	500	2	5	2 and 10	50, 1000, 1000, 50	3.20	B
F15	500	3	5	2 and 10	50, 1000, 1000, 5000	4.00	B
T16	250	2	5	2 and 10	50, 1000, 1000, 50	1.6	B
F17	500	3	18	2, 5 and 10	50, 50, 50, 50	1.75	B and C
T18	250	3	18	2, 5 and 10	50, 50, 50, 50	1.25	B
E19	85	1	18	2, 5 and 10	50, 50, 50, 50	0.85	A
T20	250	1	18	2, 5 and 10	50, 50, 50, 50	0.92	A
F21	500	1	18	2, 5 and 10	50, 50, 50, 50	1.00	A
T22	250	3	18	2, 5 and 10	50, 50, 50, 50	1.80	B
E23	85	1	18	2, 5 and 10	50, 50, 50, 50	0.75	A
F24	500	3	18	2, 5 and 10	50, 50, 50, 50	1.90	B

ment dams with clay cores, the effect of reservoir temperature is not an important factor, while in asphaltic concrete core dams, it would be. As known, nearly six to eight percent of bitumen is used in the mix design of asphalt concrete. Since the asphalt binder is a temperature dependent material, the temperature has a significant effect on the specimens' behavior. Therefore, the selection of a suitable asphalt binder to mix with aggregates is of great importance. The recommendation of selecting type B180 in cold regions like Norway and type B60 in tropical areas such as Iran are examples of this fact. Although the results of numerical analysis show that the greater part of the earthquake energy is in the frequency range of 2 to 5 Hz and all prepared specimens were imposed to loadings of 2 Hz frequency, there were also some extra tests carried out in higher frequencies of 5 and 10 Hz.

Definition of Loading

Figure 4 shows for instance, the applied cyclic loads on the samples subjected to a confining pressure of 500 kPa. The value of axial stress starts from 500 kPa, reaching 1000 kPa and then decreasing to nearly 0.0 kPa. In anisotropic conditions ($K_c = 3.0$ as an example, Fig. 5(a)),

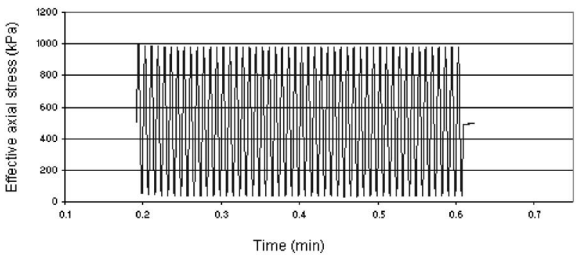

Fig. 4. Effective axial stress-loading time, $\sigma_3 = 500$ KPa and $K_c = 1.0$ (Type A)

the starting point is 1500 kPa, reaching 3000 kPa and then decreasing to nearly 0.0 kPa (cyclic load = ± 1500 kPa).

In most of previous works, regarding the confinements of setting up the loading equipment, there was no possibility of applying the two-ways loads to asphalt concrete. Consequently, the upper part of the cyclic loading records was applied to specimens (as indicated in Fig. 5(b)). This type of loading was also used for some tests in the present study.

In brief, the following types of cyclic loading used in

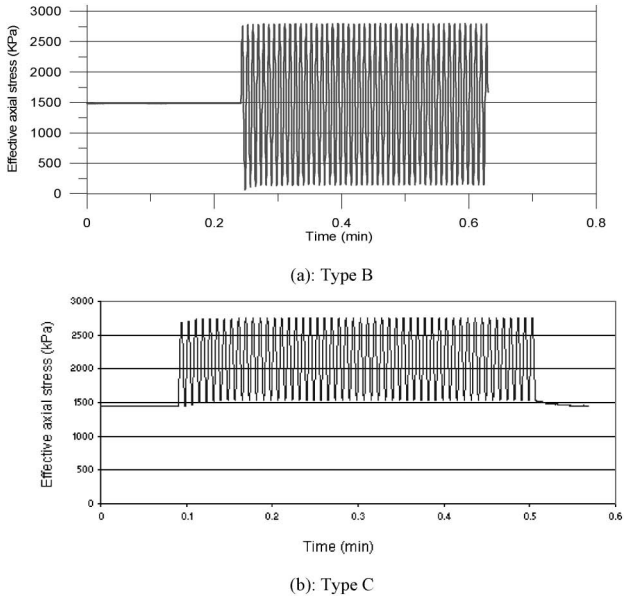

Fig. 5. Effective axial stress-loading time, $\sigma_3 = 500$ KPa, $K_c = 3.0$

this research can be noted:
Type A: Isotropic condition with symmetric cyclic loading ($K_c = 1.0$)
Type B: Anisotropic condition with non-symmetric cyclic loading ($K_c = 2.0$, 3.0)
Type C: Anisotropic condition with one-side cyclic loading

Presentation of the Results

The MTS system was scheduled to control the number of cycles. Table 2 summarizes the different parameters of these performed cyclic tests. For all specimens, the number of cycles applied at a given load level was set to 50. This number of cycles corresponds to a loading induced by an earthquake with the magnitude of 7.5 in Richter scale (Kramer, 1996). However, for tests F9 to F24 in Table 2, there were staged cycles planned and applied; for example, in test F9, 50 cycles, 400 cycles and then 50 cycles were applied. Moreover, there were small intervals (about five seconds) between each stage and the next for better observation of the asphalt concrete degradation behaviour during the cyclic loading.

Figures 6 to 11 show the hysteresis loop of the cyclic loading as examples. The hysteresis loops were plotted for the first, fiftieth, hundredths and thousandths cycles. The value of shear stress versus axial strain has been presented in these figures. The initial value of the loops was obtained from the value of axial and confining pressures. The starting point position in the hysteresis loop is defined as follows (Figs. 6 to 11):

$$\begin{cases} \text{Y position} = \text{Shear Stress in the loop} = \dfrac{\sigma_1 - \sigma_3}{2} \\ \text{X position} = \text{Shear Strain in the loop} = 0.0 \end{cases}$$

The results are described as follows in two categories; isotropic condition ($K_c = 1.0$) and anisotropic states with

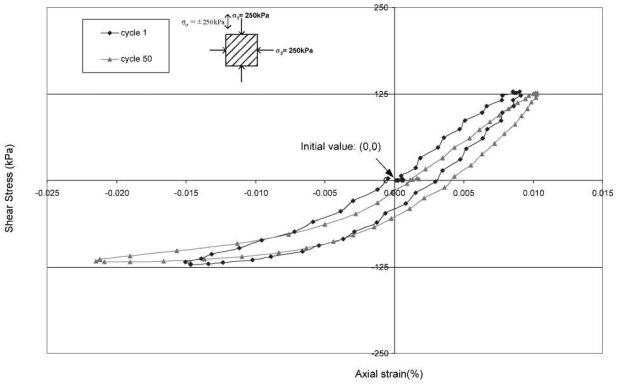

Fig. 6. Cyclic stress–strain hysteresis loop, Test T5

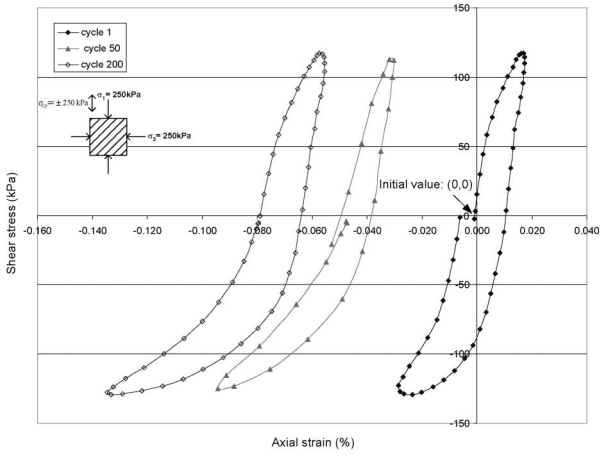

Fig. 7. Cyclic stress-strain hysteresis loop, Test T20

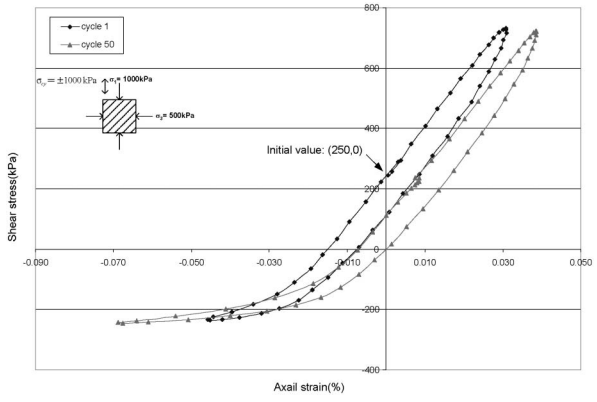

Fig. 8. Cyclic stress-strain hysteresis loop, Test F4

the values of $K_c = 2.0$ and $K_c = 3.0$.

First, for the isotropic condition (Tests T5 and T20); Figs. 6 and 7 have been plotted for instance, at two different temperatures of $T = 5°C$ and $T = 18°C$.

Figures 8 and 9 (Tests F4 and E13) are indicated for an anisotropic state with anisotropy coefficient which has the value of 2.0 ($K_c = 2.0$). In these tests, the temperature remained constant at $T = 5°C$.

Figures 10 and 11 (Tests F15 and T18) are shown for an

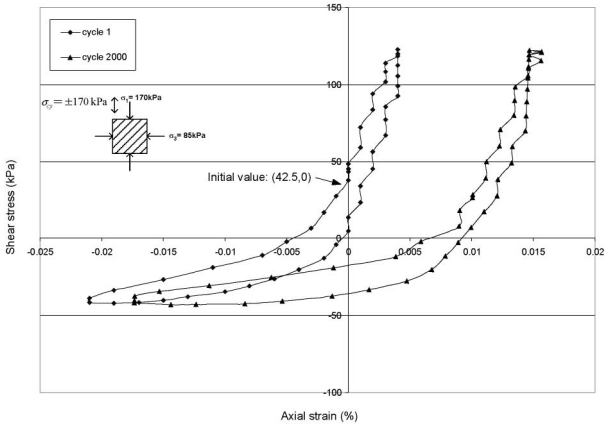

Fig. 9. Cyclic stress-strain hysteresis loop, Test E13

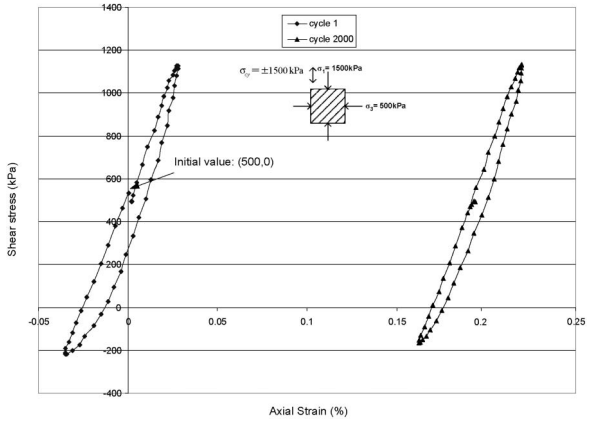

Fig. 10. Cyclic stress-strain hysteresis loop, Test F15

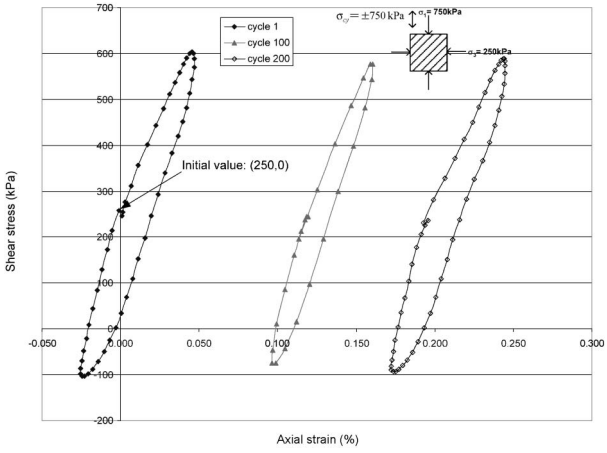

Fig. 11. Cyclic stress-strain hysteresis loop, Test T18

anisotropic state with anisotropy coefficient of 3.0 (K_c = 3.0) for two different temperatures of T = 5°C and T = 18°C.

Accuracy of Measurements

The fidelity of the results depends on the accuracy of the measurements of both stresses and strains. The obtained results are affected by two sources of error; compliance and bedding error. The compliance of the loading system, consisting of all parts (top and bottom platens and connections) between where the specimen deformation is monitored and the specimen shall be determined (Tatsuoka and Shibuya, Kohata, 1992, 1995). In the present study, errors due to apparatus compliance were evaluated with reasonable certainty by careful calibration in the laboratory. For this purpose, a cylindrical steel dummy of a similar size and length to asphalt concrete specimens was placed into the location normally occupied by the specimen where some calibration tests were performed. The Young Modulus of the dummy specimen had a minimum of ten times the modulus of the asphalt concrete (ASTM D 3999–91). Based on the obtained results, the correction coefficient was defined and used in the main tests.

On the other hand, to decrease the effect of bedding error, the surface of specimens was cut and polished with very high accuracy (Fig. 1). In addition, bedding error could cause lower stiffness in initial cycles and higher stiffness in later cycles that was not observed in hysteresis loops (Figs. 6 to 11). Therefore, the effect of bedding error can be ignored in these tests with the above considerations.

Dynamic Properties for Asphalt Concrete

In the cyclic triaxial tests, the axial stiffness and damping parameters can be directly obtained by analyzing the deviator stress-axial strain loops (Fig. 12). Cyclic triaxial tests are traditionally oriented to analyses of cyclic behavior, described by the relationship between the deviator/radial effective stress ratio (q/σ'_r) and the number of cyclic loads. The upper part of the shear stress-axial strain hysteresis curves is used to calculate the shear modulus. The following relations would then be used for this purpose:

$$E = \frac{\tau}{2\varepsilon_a}, \quad \gamma = (1+\nu)\varepsilon_a$$
$$G = \frac{E}{2(1+\nu)} \tag{6}$$

Where: τ = shear stress, ε_a = axial strain, γ = shear strain and ν = Poisson ratio.

Table 2 presents the complete information for all performed tests. The shear modulus increases from 1.5 GPa in the isotropic condition to nearly 4.0 GPa for anisotropic state with anisotropy coefficient of K_c = 3.0, at a low temperature of T = 5°C. For the higher temperature (T = 18°C), the value of shear modulus decreased to half or less as much as the mentioned values. Although the amount of shear modulus can change during cyclic loading, the 10th cycle was chosen to calculate the shear modulus. While it is observed that in the isotropic condition and low temperature, the confining stress does not have significant effect on the shear modulus, its effect increases with increase of anisotropy and temperature. By the following equation, the damping ratio (D) is calculat-

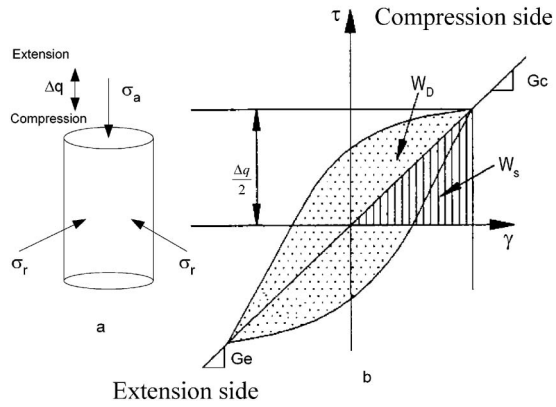

Fig. 12. Cyclic triaxial test
(a) Loads on asphalt concrete specimen
(b) Interpretation

ed as:

$$D=\frac{1}{4\pi}\frac{W_D}{W_S}\times 100(\%) \quad (7)$$

where, W_D is the damping energy in a single loading cycle and W_S is the equivalent elastic energy Based on the presented curves, the areas of the hysteresis loops and the indicated triangle were calculated. The values of the damping ratio range between 0.066 and 0.35. In the same asphalt binder percent, binder type B180 causes the decrease of the shear modulus while increasing the damping ratio compared to type B60 (Hoeg, 1993).

To show the characteristics of asphalt concrete relative to the other geotechnical materials, dynamic properties of asphalt concrete were compared with those of other geotechnical materials (Table 3). Based on the stiffness values, asphalt concrete can be laid between soft rocks and soils. In comparison with crushed-rock ($G_0\approx 2000$ to 500 MPa), round-gravel ($G_0\approx 150$ to 300 MPa), sandy-gravel ($G_0\approx 100$ to 200 MPa) and sand ($G_0\leq 100$ MPa) (Kokusho and Esashi, 1981), asphalt concrete is a stiffer material. It should be emphasized that the presented range of shear modulus is affected by the value of confining stress and void ratio. The results in Table 2 show that the amount of shear modulus for asphalt concrete ranges between 700 MPa to 4 GPa. These values correspond well to sedimentary soft rocks (Tatsuoka and Shibuya, 1992) and plastic concrete used as a cut-off wall in the embankment dams (Mahab-Ghodss, 2007). In addition, low-amplitude shear modulus for undistributed gravelly-sand (Kokusho and Tanaka, 1994) ranges between 1 GPa to 5 GPa which, can be considered to be similar to that of asphalt concrete.

On the other hand, it should be noted that the damping ratio percentage obtained in present study for the asphalt concrete is high, (especially in higher temperatures which is about 5% to 35%). Coarse material and plastic concrete can be put in this damping range.

Table 3. Comparison of dynamic parameters between asphalt concrete and the other materials

Material	G_{sec} (MPa)	Damping (%)
Asphalt concrete	700 ~ 4000	5 ~ 30
Crushed rock	200 ~ 500	2 ~ 35
Round rock	150 ~ 300	2 ~ 20
Sandy-gravel	100 ~ 200	5 ~ 20
Sand	< 100	2 ~ 15
Plastic concrete	500 ~ 5000	2 ~ 30

Investigation of Different Parameters on Dynamic Properties

Figures 13, 14 and 15 present the effect of different parameters such as confining stress, anisotropy, loading frequency, temperature and hysteresis loop shapes on the shear modulus and damping ratio. In the following paragraphs, the effects of the above-mentioned factors are described in detail.

a) Effect of anisotropy

In each part of Fig. 13, the temperature and anisotropy coefficient were fixed while the confining pressure was varied. It can be seen that the dynamic shear modulus of asphalt concrete is strongly dependent upon the shear strain. At low strain amplitudes, the shear modulus is high, but it decreases while the strain amplitude increasing. Moreover, by comparing Figs. 13(a) with (d) (at $T=$ 5°C) or Figs. 13(b) with (e) (at $T=18$°C), it can be seen that the higher the value of anisotropy coefficient, the higher the amount of shear modulus that is obtained. This is because at higher values of anisotropy state, the amount of $\sigma_{mean}(=\sigma_1+\sigma_3/2)$ increased and this was the main reason for the shear modulus augmentation.

b) Effect of temperature

Comparison of shear modulus presented at the same anisotropy coefficients in Figs. 13 ((a) and (b) at $K_c=1.0$) or Figs. 13 ((d) and (e) at $K_c=3.0$) stands for decreasing the shear modulus as the temperature increases. In addition, the temperature has an important effect on the threshold point position in G-γ curves. It is clear that with the increase in the temperature, the amount of shear modulus falls faster.

Figure 14 shows the damping ratio versus axial strain in different confining stresses at two different temperatures of $T=5$°C and $T=18$°C. Figure 14(a) shows that in comparison with shear modulus, damping ratio is not significantly dependent on the shear strain amplitude. However, its value increases gradually with increase of the shear strain level. It is observed that dependency on the strain is more distinct at the higher temperature of $T=18$°C than that at a lower temperature of $T=5$°C (Fig. 14(b)). Furthermore, by increasing the temperature, the damping ratio increases. That is because in high temperatures, viscosity of asphalt concrete causes the material to easily absorb the applied energy. Therefore, the dissipated energy in a single loading cycle and consequently the

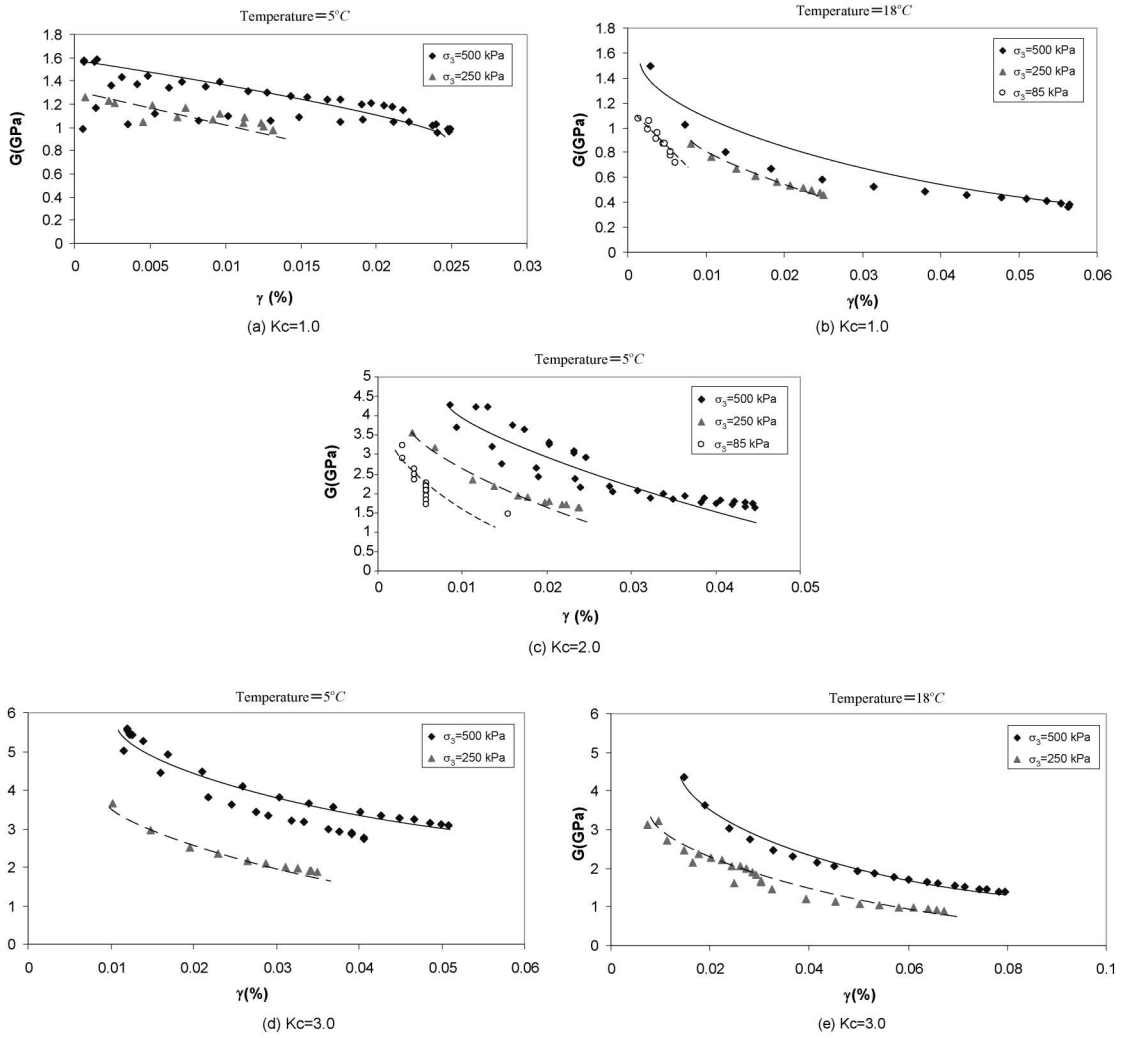

Fig. 13. Effects of σ_3 and K_c on strain-dependent modulus at two different temperatures of 5°C and 18°C

damping ratio increases.

c) Effect of confining stress

The effect of confining stress on shear modulus is also illustrated in Fig. 13. For an example in Fig. 13(a), at the constant temperature and anisotropy coefficient, the higher values of confining stress, the higher amount of shear modulus is obtained. Comparison between Fig. 13(a) and (d) (or Fig. 13(b) and (e)) shows that at a high level of anisotropy such as $K_c = 3.0$, the effect of confining stress is more distinct. In addition the threshold point occurs at higher amplitudes of shear strain in comparison with a low confining stress. This point is observed in Figs. 13(a), (c) and (d) as examples. Figure 14(a) shows that by decreasing the confining pressure from 500 kPa to 85 kPa, the damping ratio increases from 5% to 35% respectively.

d) Effect of hysteresis loops shapes

Because of the difference between the curve inclinations in compression and extension regions, two types of shear modulus, G_c and G_e, were calculated from the hysteresis loops (Figs. 6 to 11 and 12). The effects of confining stress (Fig. 15(a)), anisotropy coefficient and the temperature (Figs. 15(b) and (c)) were plotted separately for these two types of modulus. It shows that the value of shear modulus in compression region is more than two times of the value in extension side in the same temperature and confining stress ($G_c \geq 2G_e$). It is clearly seen in Fig. 15(c) that with increasing confining stress and/or anisotropy coefficient at the constant temperature, the values of G_c and G_e increase. Moreover, Fig. 15(b) shows that the values of G_c and G_e decrease at the higher temperature.

e) Effect of reversal coefficient (r_c)

Reversal Ratio is introduced by the reversal coefficient (r_c), which is the proportion of the positive portion in applied cyclic shear stress to the whole domain of the shear stress. The effect of stress reversal ratio in the G-log N diagram has been also studied, (where N is the number of applied cycles.)

Figure 16 shows the G-log N curves for different values of r_c. It is observed that the larger the value of r_c, the higher is the curve in the G-log N diagram. This means the potential for degradation increases when the extension mode has become more predominant. In addition, this figure shows that in lower values of r_c (such as $r_c = 0.5$), the amount of degradation for shear modulus is less than that of higher values ($r_c = 0.85$). In addition, this

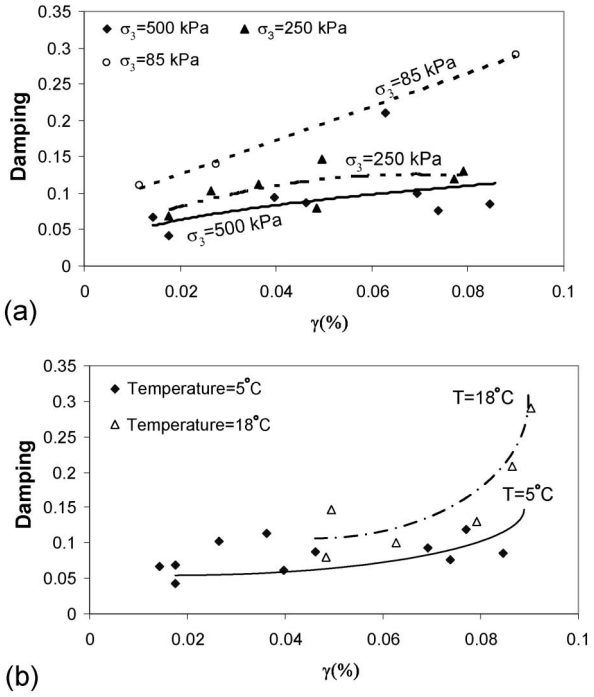

Fig. 14. Effects of confining stress and temperature on strain-dependent damping ratio

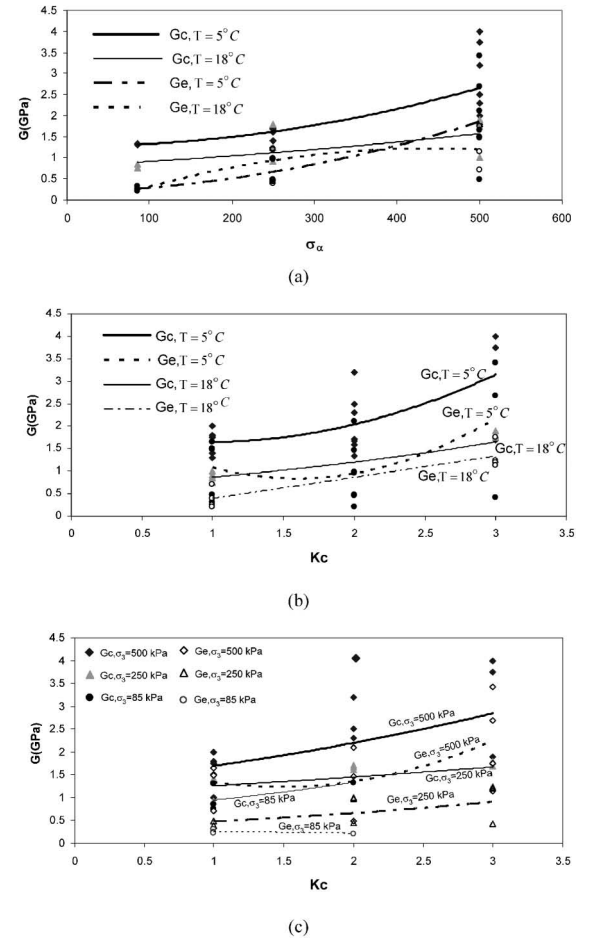

Fig. 15. Comparison between shear modulus in extension and compression states at two temperatures of 5°C and 18°C with different confining stresses

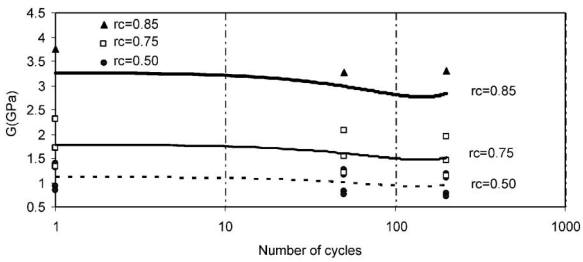

Fig. 16. *G*-Log *N* curves for different values of r_c

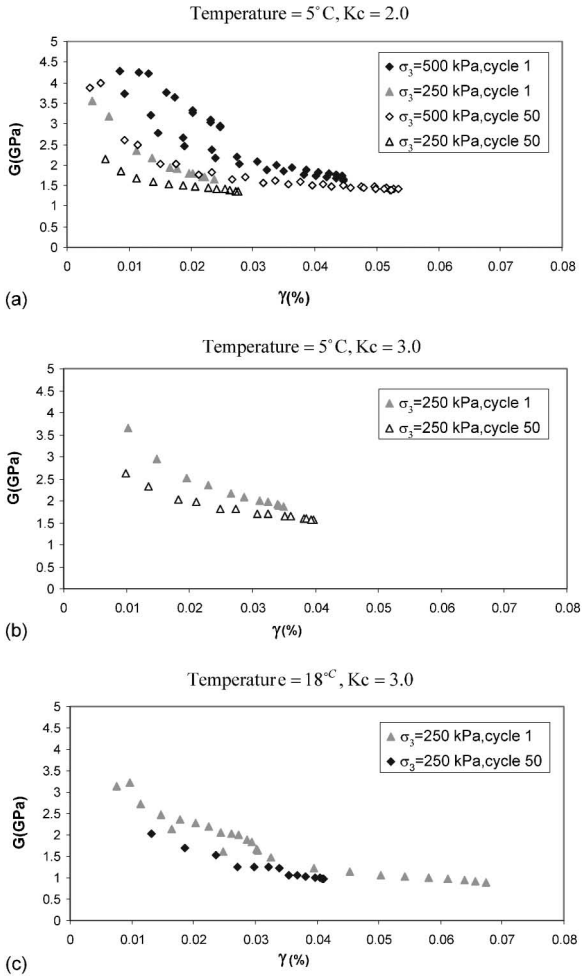

Fig. 17. Effect of cycles number on shear modulus

figure shows that increasing the number of cycles caused decrease of shear modulus.

f) Effect of number of cycles

Figure 17 presents the effect of the number of cycles on modulus reduction behavior at different confining stresses, anisotropy coefficients and temperatures. The value of shear modulus is plotted in the first and fiftieth cycles. It is seen that holding constant the values of confining stress, anisotropy coefficient and temperature, by increasing the number of cycles, the amount of shear modulus decreases (Figs. 17(a), (b) and (c)). This reduction behavior is more distinct at a low level of shear strain. In addition, the shear modulus reduction behavior is more

prevailing in a low confining stress ($\sigma_3 = 250$ kPa) than higher confining stresses (Fig. 17(a) for an example). At the same temperature and confining stress, comparison between Figs. 17(a) and (b) shows that with increase of anisotropy coefficient, the effect of the number of cycles decreases. In other words, in the same cycle number, the specimens degradation with a higher value of anisotropy coefficient ($K_c = 3.0$) is less than that of $K_c = 2.0$. Figures 17(b) and (c) shows that the value of temperature has a significant influence on the dynamic properties of asphalt concrete between the first and fiftieth cycles. Indeed, in high temperatures, the threshold point for G-γ curves occurs at a low level of shear strain.

Strain Values and Specimens Cracking

In the present research, because of using ASTM standards at the laboratory, the external transducers were used to measure deformations. Though the research developments in advanced triaxial equipments (e.g., Tatsuoka et al., 1992, 1995) have shown that shear strains as low as 0.001% can be resolved in static (e.g., Goto et al., 1991) and cyclic triaxial tests by using local displacement transducers, however, with proper mounting as well as carefully calibrating the high resolution transducer and by considering the effects of equipment compliance and bedding error (ASTM D 3999–91), the reliability of the results can be put in an acceptable range.

As expected, the value of strain was very small. Hence, a very high precision electronic displacement transducer was used to record the value of displacement during the cyclic loads. According to ASTM D 5311–92 and 3999–91, displacement measuring devices such as LVDT may be used if they have an accuracy of $\pm 0.02\%$ of the initial specimen height. Since specimens height in the present study was 200 mm, the accuracy of ± 0.04 mm had to be the minimum required accuracy for the used LVDT. The LVDT used at the laboratory satisfied this condition very well and other criteria suggested in the ASTM standards.

Figure 18 summarizes the axial strain ($\Delta\varepsilon$) for performed tests at the end of the loading in different frequencies. In high speeds of cyclic loading, the strain values decrease ($F = 5$ Hz and 10 Hz). Since, in higher loading speeds, asphalt concrete cannot show its flexibility and viscosity behavior very well, consequently the axial strain values are less than those of low speeds. Good compaction of the samples was one of the reasons of rather small displacements. In addition, the value of axial strain increases with the increase of confining pressure. With reference to Figs. 13 and 15, it is obvious that the temperature has the largest effect on the strain values. As expected, the higher the value of temperature, the greater is the amount of axial strain.

After the cyclic tests, specimen surfaces were well inspected. In addition, some specimens were cut horizontally and vertically to investigate the cracking in the interior surfaces (Fig. 19). There was not any sign of cracks, even after 10000 cycles. This shows a good response of the asphalt concrete specimens resisting against cyclic loads.

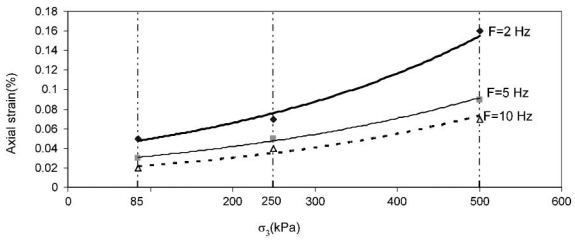

Fig. 18. σ_3-$\Delta\varepsilon$ curves for different values of frequency

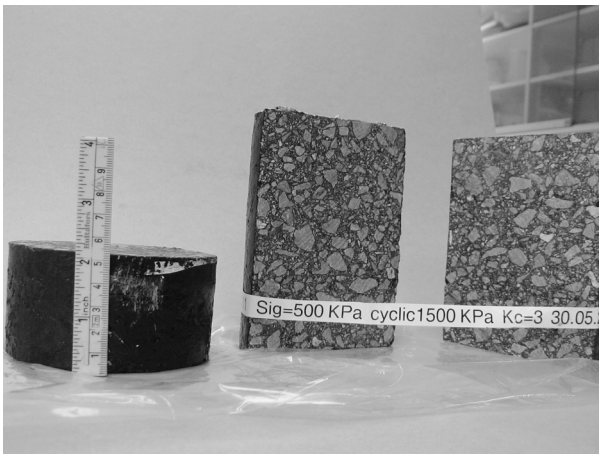

Fig. 19. Cross setion of the specimen after 10000 cycles

Degradation of the Asphalt Concrete Specimens

The shape and inclination of the hysteresis curves would be good criteria to investigate the material degradation. Hence, the average inclination of the first hysteresis loop was calculated and compared with the slopes of other loops. This comparison showed that by increasing the number of cycles, the amount of curves inclination decreased (Figs. 6 to 11 and 17). It was also observed that the value of shear modulus was gradually decreasing during the cyclic loading. Some tests were run with thousands of load cycles to study whether there is a long-term degradation (fatigue) phenomenon which was not found noticeable to be the case up to 10000 cycles (Fig. 19).

Figures 6 to 11 show that the banana shape was seen in the extension mode. In the presented figures (Figs. 6 to 11), the curves' inclination in extension mode is less than that of the compression mode. Therefore during the cyclic triaxial tests, specimen strength reaches the failure line in extension mode. Consequently the values of axial strain increases. With the application of compression loads, the specimens' behaviour is changed. However, some residual strain remains. It is one of the explications to describe the banana shape in the extension region. Anisotropy in asphalt concrete; because of the direction of compaction, is another reason to make the banana looking shape in the extension mode.

Description of Different Behaviors of the Asphalt Concrete

During the cyclic triaxial tests of asphalt concrete, two different behaviors were observed; Extension and Compression, which are summarized in Table 4. According to this table, the extension behavior may occur in a low level of confining stress such as near the dam crest and hence this part of dam is more vulnerable during the cyclic loading.

Table 4 shows that during the cyclic tests with higher values of K_c, the compression behavior occurs. Although the amount of strain is very small, the loads compress the material. For anisotropic condition, changing the temperature, confining pressure and loading frequency affect the strain values only and do not alter the general behavior (compression) of the specimens.

As mentioned above, the extension behavior is only seen in the isotropic state ($K_c = 1.0$). Increasing the temperature or decreasing the confining pressure are the main factors causing extension. In this state, compression behavior was just seen at a low temperature ($T = 5°C$) and high confining pressures ($\sigma_3 = 250,500$ kPa) while extension behavior was seen in other cases.

Since the extension behavior is just observed at $K_c = 1.0$, the effects of temperature and confining stress on the general behavior of asphalt concrete is explained more in the following paragraphs:

a) Effect of temperature (in isotropic condition)

The cyclic tests were performed at two different temperatures, $T = 5°C$ and $T = 18°C$. As presented in Table 4, in the constant confining stress, extension behavior occurred in a higher temperature. For the reason that in a higher temperature, the effect of material viscosity is more distinct and the increment of confining pressures can not substantially affect the compression behavior of the material. It should be noted that the prepared specimens for the cyclic tests are bitumen rich. The so called ''Rich'' is used for the specimens with the high percentage of the bitumen. In a low temperature ($T = 5°C$), the sample behaves rigidly. With increasing temperature, the compaction, mixture quality of aggregate with bitumen and the particles interlocking are more influential.

b) Effect of confining stress (in isotropic condition)

The cyclic tests were performed in three different confining pressures, $\sigma_3 = 85$, 250 and 500 kPa. By increasing the confining pressure, the compression behavior is more distinct than that of extension; this is specifically more remarkable at low temperatures. At the temperature of $T = 18°C$, in all confining pressures, the extension behavior was observed while at the temperature of $T = 5°C$, this behavior was just seen at $\sigma_3 = 85$ kPa. In other words, in a low level of confining pressure ($\sigma_3 = 85$ kPa), only the extension behavior is observed and the temperature effect can be negligible.

Near the dam crest the amount of confining pressure is not considerable. It is also well established that this part of the core is very vulnerable during the earthquake. Therefore, special control of the dam during the construction on this region would be necessary.

Table 4. Different types of asphalt concrete behavior during the cyclic loading

σ_3 (kPa)	$K_c = 1.0$		$K_c = 2.0$	$K_c = 3.0$	
	$T = 5°C$	$T = 18°C$	$T = 5°C$	$T = 5°C$	$T = 18°C$
85	Extension	Extension	Compression	Compression	Compression
250	Compression	Extension			
500	Compression	Extension			

POST-CYCLIC BEHAVIOUR OF THE ASPHALT CONCRETE SAMPLES

After an earthquake shocking, the structures should retain their efficiency and operate normally. The mentioned period is titled the ''*post-cyclic operation time*''. To simulate this occurrence, after completing the cyclic tests, some specimens were selected to be imposed by monotonic loading. The post-cyclic monotonic stress-strain curve would be compared to the corresponding curve for the specimens not first subjected to cyclic load-

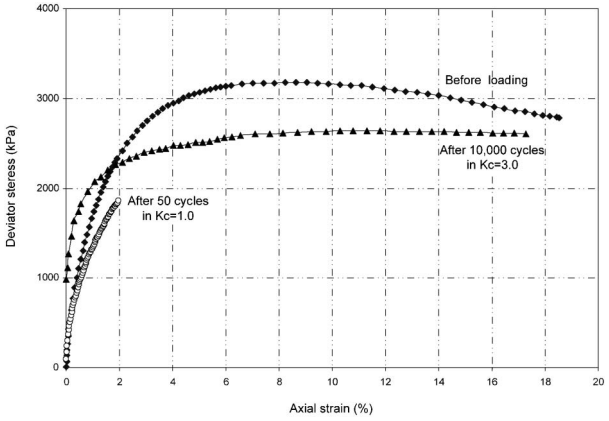

Fig. 20. Post cyclic behaviour (stress-strain curve), $\sigma_3 = 500$ KPa, $T = 5°C$

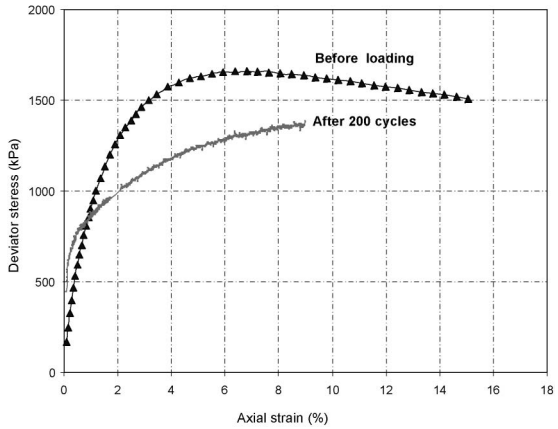

Fig. 21. Post cyclic behaviour (stress-strain curve), $\sigma_3 = 250$ KPa, $T = 18°C$

ing, to study any sign of material degradation due to the cyclic loading. Figure 20 shows the comparison of the stress-strain curve for one of the specimens before and after the cyclic loading at a low temperature of $T = 5°C$. The cyclic tests were performed at different anisotropy states ($K_c = 1.0$ and $K_c = 3.0$). The amount of degradation is nearly 15 percent at the pick point of the curve. In addition, the figure shows a similar overall behavior for the samples before and after subjecting to cyclic loading.

Figure 21 shows the monotonic test results for the specimen after cyclic loading in a high temperature ($T = 18°C$). The figure shows the same behavior trend for the tests before and after the cyclic loading in a high temperature of $T = 18°C$ like $T = 5°C$.

It can be concluded that the asphalt concrete retains its efficiency after cyclic loads application and the post-cyclic behaviour of this material is still suitable.

SUMMARY AND CONCLUSIONS

Lack of high quality experimental data on the asphalt concrete subjected to earthquake loading was the main incentive to perform this research. The outcome of the present study shows the behavior of asphalt concrete under cyclic loading. During the design procedure, it is necessary to have exact material properties to control the dam stability.

The results obtained from the present study can be summarized as follows:

- Triaxial monotonic tests were performed to study the stress-strain behavior of asphalt concrete material. Strength and stiffness increased with higher confining stress, σ_3. Based on the monotonic tests results, the Young's secant modulus at 1% axial strain is proposed to be $E_{1\%} = A \times \sigma_0^{0.18}$. In addition, higher confining stresses imposed on the specimens caused lower dilatancy and volume expansion during shearing.
- In the cyclic triaxial tests, fifty cycles were imposed on the specimens to simulate earthquake excitations. In some cases, the cyclic loads were continued to thousands of cycles. However, there was no significant degradation detected on the specimen behavior. No cracks on the specimen surfaces were detected, even after 10000 cycles.
- Many factors influence the dynamic properties of the asphalt concrete, such as confining stress, stress anisotropy, loading frequency and temperature. The effects of the mentioned factors are more distinct on the shear modulus than on the damping ratio. The dynamic shear modulus of asphalt concrete is strongly dependent on the shear strain.
- The damping ratio increases with the increase of dynamic strain at lower stress ratios (K_c), while being constant at higher stress ratios.
- The cyclic strain values were less than 0.20% for the performed tests. The cyclic amplitude remains constant even for a large number of cycles. The smallest values of strain occur for low temperatures and high frequency loading.
- After the completion of cyclic loading, monotonic tests were carried out on the samples to investigate the post-cyclic behaviour. The results show that the asphalt concrete behaves much the same way as prior to cyclic loading. However, by increasing the temperature, the amount of degradation increases. Post-cyclic behaviour shows that the reduction in shear strength after cyclic loading is insignificant. The increase of permeability only occurs when fissures get opened near the failure level in monotonic loading.
- This study shows that asphaltic concrete is resistant to earthquake excitations. The earthquake has to be very strong to cause any detrimental cracking or material degradation of the properties of a ductile asphaltic concrete core in embankment dam.

ACKNOWLEDGMENT

The present research was supported by the Iran Water Resources Management Organization (IWRMO) and Mahab-Ghodss consulting engineers in Iran and the contractor Kolo-Veidekke in Norway. The authors appreciate the assistance of laboratory employees at the Norwegian Geotechnical Institute and Kolo-Veidekke during the experimental work.

NATATION

The following terms are utilized in this research:

e: *void ratio of specimens*

n: *porosity of specimens*

υ: Poisson ratio

σ_3: *confining stress*, is a pressure applied into the triaxial cell

σ_1: *axial stress*, is applied in the axial direction of the specimen, while lateral stress is applied in the radial direction of the specimen

σ_d: *deviator stress*, is the difference between major and minor principal stresses in a triaxial test

K_c: *anisotropic stress ratio*, is calculated by dividing the axial stress by lateral stress ($K_c = \sigma_1/\sigma_3$)

Reversal ratio, is introduced by the reversal coefficient (r_c), which is the relative value of positive portion of applied cyclic shear stress to the whole domain of shear stress

G: *shear modulus*, is calculated from hysteresis loops. G_c and G_e are defined for the compression and extension regions inclination, respectively

D: *damping ratio*, is carried out from hysteresis loops

Degradation, is the reduction amount of material strength

Threshold point, is the point that separates the constant and falling parts of the G-γ curve

Compression behavior, is the shortening of the specimen's height under the cyclic loading

Extension behavior, is the elongation of the specimen's height under the cyclic loading

REFERENCES

1) Baron, W. F. and Van Asbeck (1955): *Bitumen in Hydraulic Engineering*, Shell Petroleum Co., Ltd., **1**, London, England.
2) Breth, H. and Schawab, H. H. (1973): Zur Eignung des asphaltbetons fur die Innendictung von Staudammen, *Wassewirtschaft*, **69**, Heft 11, 348–351, Stuttgart, Germany.
3) Creegan, P. and Monismith, C. (1996): *Asphaltic Concrete Water Barriers for Embankment Dams*, ASCE Press.
4) Dunnicliff, J. (1996): *Geotechnical Instrumentation for Monitoring Filed Performance*, 2nd Edition.
5) Feizi-Khankandi, S., Mirghasemi, A. A. and Ghanooni, S. (2004): 3-D seismic analysis of asphaltic concrete core rockfill dams, *ICGE Conference*, 220–225, UAE.
6) Ghanooni, S. and Mahin-roosta, R. (2002): Seismic analysis and design of asphaltic concrete core embankment dams, *Journal of Hydropower and Dams*, **6**, 75–78.
7) Goto, S., Tatsuoka, F., Shibuya, S., Kim, Y. S. and Soto, T. (1991): A simple gauge for local small strain measurements in laboratory, *Soils and Foundations*, **31**(11), 169–180.
8) Gurdil, A. F. (1999): Seismic behavior an Asphaltic Concrete core dams, *Proc. 1st Symposium on Dam Foundation*, Antalya, Turkey.
9) Hoeg, K. (1993): *Asphaltic Concrete Cores for Embankment Dams*, Norwegian Geotechnical Institute, Oslo, Norway.
10) Hoeg, K. (2005): Earthquake resistance of Asphaltic concrete core, *Report No. 20051031–1*, Oslo, Norway.
11) Hoeg, K., Valstad, T., Kjaernsli, B. and Ruud, A. M. (2007): Asphalt core embankment dams: recent case studies and researches, *Journal of Hydropower and Dams*, **13**(5), 112–119.
12) ICOLD Press (1982, 1992): *Bituminous Cores for Earth and Rockfill Dams*, Bulletin 42 and 84.
13) International Navigation Association Press (1997): *Seismic Design Guidelines for Port Structure*, working group No. 34 of the Maritime Commission International Navigation Association.
14) Japanese Geotechnical Society (2000): *Standards of Japanese Geotechnical Society for Laboratory Shear Test*, Japan.
15) Kokusho, T. and Esashi, Y. (1981): Cyclic triaxial test on sands and coarse materials, *Proc. 10th ICSMFE*, (Quoted by Ishihara 1986), Stockholm, Sweden.
16) Kokusho, T. and Tanaka, Y. (1994): Dynamic properties of gravel layers investigated by in-situ freezing sampling, *Proc. Ground Failure under Seismic Conditions*, ASCE Annual Convention, Atlanta, USA.
17) Kramer, S. (2007): Geotechnical earthquake engineering, *Cut of Wall for Gotvand Dam*, Prentice Hall, Inc, USA, 1996–Mahab-Ghodss report, Iran.
18) Meintjes, H. A. C. and Jones, G. A. (1999): Dynamic analyses of the new cores dam, *Proc. 12th Regional Conference for Africa on SMGE*, Durban, South Africa.
19) Nakamura, Y., Okumura, T., Narita, K. and Ohne, Y. (2004): Improvement of impervious asphalt mixture for high ductility against earthquake, *Proc. 4th International Conference on Dam Engineering*, 18–20, China.
20) Ohne, Y., Nakamura, Y., Okumura, T. and Narita, K. (2002): Earthquake damage and its remedial measure for earth dams with asphalt facing, *Proc. 3rd US-Japan Workshop on Earthquake Engineering for Dams*, 15–26, Japan.
21) Salemi, S. (2005): Dynamic behavior investigation of asphaltic concrete core Rockfill Dams, IUST University, *PhD Dissertation*, Iran.
22) Tatsuoka, F. and Shibuya, S. (1992): Deformation characteristics of soils and rocks from field and laboratory tests, *Report of the Institute of Industrial Science*, University of Tokyo.
23) Tatsuoka, F. and Kohata, Y. (1995): Stiffness of hard soils and soft rocks in engineering applications, *Report of the Institute of Industrial Science*, University of Tokyo.
24) Valstad, T., Selness, P. B., Nadim, F. and Aspen, B. (1991): Seismic response of a rockfill dam with an asphaltic concrete core, *Journal of Water Power and Dam Construction*, **43**, 1–6.
25) Wang, W. (2005): *Cyclic Tests on Asphalt Concrete*, Xi'an University Press, China.
26) Wang, W. and Hoeg, K. (2002): Effects of compaction method on the properties of asphalt concrete for hydraulic structures, *International Journal on Hydropower and Dams*, **9**(6), 63–71.